Decoherence of a singlet-triplet superposition state under dipolar interactions of an uncorrelated environment

Patrick Vorndamme and Jürgen Schnack
Department of Physics, Bielefeld University, 33615 Bielefeld, Germany
(Dated: February 3, 2020)

Recently, it was shown that by means of an scanning tunneling microscope it is experimentally possible to stimulate clock transitions between the singlet and the non-magnetic triplet state of a Heisenberg-coupled spin dimer [Bae et al., Sci. Adv. 4, eaau4159 (2018)]. This leads to more strongly protected clock transitions while ordinary ones only provide first-order protection against magnetic noise. However, large decoherence times of clocklike states normally refer to ensembles of spins which do not dephase. In the cited experiment, only one single dimer is manipulated and not an ensemble. For this reason, we simulate how a single dimer behaves in an environment of other spins which couple to the dimer via dipolar interactions. We perform unitary time evolutions in the complete Hilbert space, including dimer and a reasonably large environment. We will see that for a weak environment, this approach confirms long decoherence times for the clocklike state, but with stronger couplings this statement does not hold. As a reference, we compare the behavior of the dimer with other, non-clocklike, superposition states. Furthermore, we show that the internal dynamics of the bath plays an important role for the decoherence time of the system. In a regime where the system is weakly coupled to the bath, stronger interactions among environmental spins worsen the decoherence time up to a certain degree, while if system and bath are strongly coupled, stronger interactions in the environment improve decoherence times.

I. INTRODUCTION

To perform quantum computing, it is necessary to have building blocks that are individually controllable and whose superposition states have long decoherence times. Spin systems that exhibit clock transitions are promising candidates at least for the last property [1–4]. Such clock transitions mean a stimulation between two energy eigenstates $|E_1\rangle$ and $|E_2\rangle$ of the system which are independent of the external magnetic field at least to first order [2]. This leads to a precession of the phase difference in a superposition of these two states with a frequency $\omega = E_1 - E_2$ which is thus also independent of the external magnetic field. When an experimenter excites an ensemble of such systems, all spins precess at the same frequency ω and do not dephase, regardless of local magnetic field fluctuations. Experimentally, this results in large T_2^* times.

In this paper we investigate the decoherence behavior of a single spin dimer which is dipolar coupled to a bath of environmental spins, motivated by the experiment described in [1]. Regarding decoherence this is a completely different scenario compared to dephasing of an ensemble of spins. As an approximation of the exact environment in the experiment we use a model system in which the environmental spins are randomly distributed on a spherical surface around the spins of the dimer. Therefore, the absolute values of our decoherence times are not realistic, but we can make relative statements in the sense that scenario A has a much longer decoherence time than scenario B, using our environment as a test bed.

Generally, local magnetic field fluctuations can have many sources. Beyond an inhomogeneity in the external field, referred to as non-intrinsic decoherence, intrinsic effects such as dipolar interactions of near nuclei are important [5]. But not only that, for molecular spin clusters it was shown that interactions with neighboring electronic spins play an important role, too [6]. Thus, we investigate in our model both cases: strong and weak magnetic moments of the environmental spins.

Figure 1 illustrates the system we are interested in, a Heisenberg coupled spin dimer with $s_1 = s_2 = 1/2$ and thus four energy levels. Two of them are completely independent of the external magnetic field, not only to first order. We will refer to a superposition between these two states as our clock like scenario. Experimentally, it is possible to create and manipulate these superpositions [1]. In view of this, such systems are individually controllable; this meets an important criterion for the usability in the context of quantum computing as pointed out in the beginning. In the experiment the dimer consists of two titanium atoms, a localized time-dependent magnetic field was realized by means of an STM tip. The tip moved one atom in an inhomogeneous magnetic field. In this way, the atom experienced a time-dependent magnetic field. A small difference in the Landé factors of the two atoms was also compensated by the tip.

As a side note we want to point out that manipulation of single (molecular) spins is usually difficult. Magnetically this is possible by means of an STM. But in the area of spintronics much research is also being devoted to how individual spins can be manipulated by means of time-dependent electric fields as an alternative approach [7, 8].

The paper is organized as follows. In Section II we introduce the theoretical model. In Section III we explain the different scenarios we investigate for the initial state of the dimer and how we prepare the environment. We also point out why decoherence is a process for which no energy exchange between system and environment is

needed; it therefore differs from relaxation and thermalization. In Section IV we show our numerical results. The article closes with a discussion in Section V.

II. MODEL

The Hamiltonian of our model consists of three parts

$$\underset{\sim}{H} = \underset{\sim}{H}_S + \underset{\sim}{H}_{SE} + \underset{\sim}{H}_E \ . \tag{1}$$

The first part $\underset{\sim}{H}_S$ (system Hamiltonian) describes the spin dimer and contains Heisenberg and Zeeman terms

$$\underset{\sim}{H}_S = J\,\underset{\sim}{\vec{s}}_1 \cdot \underset{\sim}{\vec{s}}_2 + g_S \mu_S B(\underset{\sim}{s}_1^z + \underset{\sim}{s}_2^z) \ . \tag{2}$$

The magnetic field B is constant and points into z-direction. The coupling constant J is chosen to be antiferromagnetic ($J = 9.425$ K, with $\hbar = k_B = 1$) and of the same order of magnitude as measured in the experiment [1]. The magnetic interaction strength $g_S\mu_S = 1.3434$ K/T is chosen to be the same as for free electrons. The dimer consists of two spins $s_1 = s_2 = 1/2$ so that $\underset{\sim}{H}_S$ has four energy eigenvalues. The spins couple either to total spin $S = 0$ (singlet), or to a spin $S = 1$ (triplet). As marked in Fig. 1, the eigenstates of the singlet and the non-magnetic triplet state are given by

$$|\psi^{\pm}_{Clock}\rangle = \frac{1}{\sqrt{2}}\left(|\uparrow\downarrow\rangle \pm |\downarrow\uparrow\rangle\right) \ , \tag{3}$$

and the other two states of the triplet are provided by the polarized states $|\uparrow\uparrow\rangle$ and $|\downarrow\downarrow\rangle$.

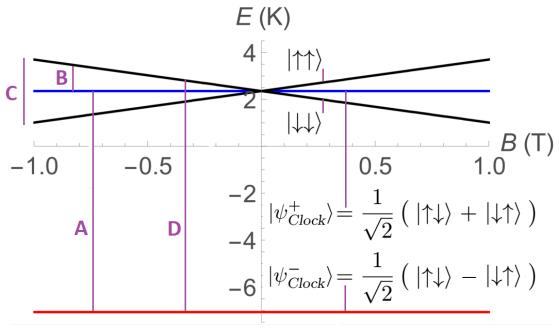

FIG. 1. Energy eigenvalues of $\underset{\sim}{H}_S$. The singlet state is shown in red, the non-magnetic triplet state in blue and the other two triplet states in black.

The second part $\underset{\sim}{H}_{SE}$ of Hamiltonian Eq. (1) contains dipolar interactions between dimer and $(N-2)$ environmental spins

$$\underset{\sim}{H}_{SE} = \sum_{i=1}^{2}\sum_{j=3}^{N} \frac{A_1}{r_{ij}^3}\left(\underset{\sim}{\vec{s}}_i \cdot \underset{\sim}{\vec{s}}_j - \frac{3(\underset{\sim}{\vec{s}}_i \cdot \vec{r}_{ij})(\underset{\sim}{\vec{s}}_j \cdot \vec{r}_{ij})}{r_{ij}^2}\right) \tag{4}$$

with constant

$$A_1 = \frac{\mu_0 g_S \mu_S g\mu}{4\pi} \ . \tag{5}$$

We will use the factor $g\mu$ as tunable parameter for the dipolar interaction strength of the environmental spins and therefore the coupling between system and environment.

The last part $\underset{\sim}{H}_E$ contains dipolar interactions between different environmental spins and their Zeeman terms

$$\underset{\sim}{H}_E = \lambda \sum_{i=3}^{N}\sum_{j=i+1}^{N} \frac{A_2}{r_{ij}^3}\left(\underset{\sim}{\vec{s}}_i \cdot \underset{\sim}{\vec{s}}_j - \frac{3(\underset{\sim}{\vec{s}}_i \cdot \vec{r}_{ij})(\underset{\sim}{\vec{s}}_j \cdot \vec{r}_{ij})}{r_{ij}^2}\right) + \sum_{i=3}^{N} g\mu(B + \Delta B_i)\underset{\sim}{s}_i^z \tag{6}$$

with constant

$$A_2 = \frac{\mu_0 (g\mu)^2}{4\pi} \tag{7}$$

and magnetic fluctuations ΔB_i at the individual positions of the environmental spins. We found that in our scenarios these inhomogeneities make no difference; we therefore apply in the following $\Delta B_i = 0\ \forall i$. The factor λ in Hamiltonian Eq. (6) allows us to scale the dipolar interactions among environmental spins only, without changing $\underset{\sim}{H}_{SE}$. Increasing the value of λ is comparable to a situation where the environmental spins are closer together and therefore interact stronger.

In case of dipolar interactions we need to choose spatial coordinates of all spins. Altogether we choose $N = 20$ spins of which $(N-2)$ are environmental spins. We arrange each half of them randomly around the two spins of the dimer on a spherical surface with radius $R = 1.5$ Å. The model is illustrated in Figure 2.

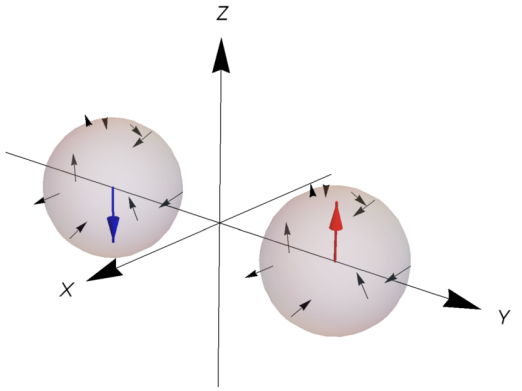

FIG. 2. Symbolic visualization of the investigated model. The two spins of the dimer are shown in red and blue and there are nine environmental spins on a spherical surface around both of them.

We pretend the two spins of the dimer s_1 and s_2 far apart ($r_{ij} \to \infty$), so that with respect to the dipolar interactions the two clusters of environmental spins do not mutually interact. This simplifies the calculation and should not be unphysical, since the dipolar interactions

decrease with r_{ij}^3. This trick also allows us to diagonalize the Hamiltonian $\underset{\sim}{H}_S + \underset{\sim}{H}_E$ (without $\underset{\sim}{H}_{SE}$) because the effective Hilbert space is smaller and we can show the energy spectrum of system and environment. But in order to perform time evolution including $\underset{\sim}{H}_{SE}$ the Hilbert space is too large to diagonalize the Hamiltonian, and we rely on other numerical methods.

Figure 3 shows the energy spectrum of $\underset{\sim}{H}_E$ with parameters $B = -1$ T, $g\mu = 0.6717$ K/T and $\lambda = 1$. Figure 4 shows the combined spectrum of $\underset{\sim}{H}_S + \underset{\sim}{H}_E$ with the same parameters. Most energy eigenvalues are centered around the singlet and the triplet region of the dimer, which gives two peaks in the distribution of energy values but also energies in between. Therefore, the interaction $\underset{\sim}{H}_{SE}$ will cause transitions between levels of this spectrum when the system is time-evolved with the full Hamiltonian (1), even for small interactions $\underset{\sim}{H}_{SE}$.

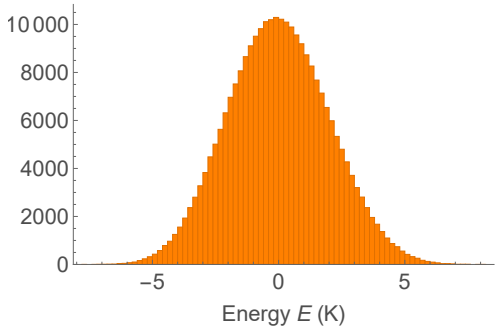

FIG. 3. Histogrammed number of energy eigenvalues of environmental Hamiltonian $\underset{\sim}{H}_E$ at $B = -1$ T. The magnetic interaction strength is chosen to be $g\mu = 0.6717$ K/T with scaling parameter $\lambda = 1$. The total number of energy eigenvalues is 2^{18}.

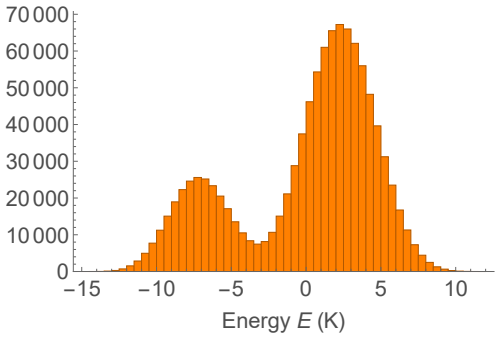

FIG. 4. Histogrammed number of energy eigenvalues of Hamiltonian $\underset{\sim}{H}_S + \underset{\sim}{H}_E$ at $B = -1$ T. The magnetic interaction strength is chosen to be $g\mu = 0.6717$ K/T with scaling parameter $\lambda = 1$. The total number of energy eigenvalues is 2^{20}.

In general, our approach is very similar to central spin models with the difference that we have two spins of interest in the center [9, 10].

III. PREPARATIONS

In all following calculations we initialize the total state in a product

$$|\psi(t=0)\rangle = |\psi_S\rangle \otimes |\psi_E\rangle \tag{8}$$

of dimer and its environment. As initial state of the dimer we investigate different scenarios. We choose between four initial states $|\psi_S\rangle$ that are all superpositions of eigenstates of $\underset{\sim}{H}_S$

$$\text{A: } |\psi_S\rangle = \frac{1}{\sqrt{2}}\left(|\psi^+_{Clock}\rangle + |\psi^-_{Clock}\rangle\right) = |\uparrow\downarrow\rangle \tag{9}$$

$$\text{B: } |\psi_S\rangle = \frac{1}{\sqrt{2}}\left(|\psi^+_{Clock}\rangle + |\downarrow\downarrow\rangle\right) \tag{10}$$
$$= \frac{1}{2}|\uparrow\downarrow\rangle + \frac{1}{2}|\downarrow\uparrow\rangle + \frac{1}{\sqrt{2}}|\downarrow\downarrow\rangle$$

$$\text{C: } |\psi_S\rangle = \frac{1}{\sqrt{2}}\left(|\uparrow\uparrow\rangle + |\downarrow\downarrow\rangle\right) \tag{11}$$

$$\text{D: } |\psi_S\rangle = \frac{1}{\sqrt{2}}\left(|\psi^-_{Clock}\rangle + |\downarrow\downarrow\rangle\right) \tag{12}$$
$$= \frac{1}{2}|\uparrow\downarrow\rangle - \frac{1}{2}|\downarrow\uparrow\rangle + \frac{1}{\sqrt{2}}|\downarrow\downarrow\rangle\,.$$

To make a statement if the initial state of the dimer in scenario A has a long decoherence time we need to compare it with a reference in the same model environment. Our reference will be the scenarios B, C and D which are non-clocklike superpositions. Due to dipolar interactions with the environmental spins, the state Eq. (8) will not remain a product state: system and environment will entangle.

Since our Hamiltonian is time-independent, time evolution is given by

$$|\psi(t)\rangle = \underset{\sim}{U}(t)\,|\psi(0)\rangle = e^{-i\underset{\sim}{H}t}\,|\psi(0)\rangle \tag{13}$$

with time evolution operator $\underset{\sim}{U}(t)$ and full Hamiltonian $\underset{\sim}{H}$, Eq. (1). We calculate the evolution with a Suzuki-Trotter product expansion numerically exact [11]. As the initial state of the environment $|\psi_E\rangle$ we choose a random state with Gaussian distributed coefficients, both for real and imaginary parts. In this way, we reach all of the possible states with the same probability [12–15]. The state $|\psi_E\rangle$ is maximally uncorrelated, also referred to as an infinite temperature state.

In general, the state of the environment can have a considerable impact on the decoherence behavior of the system as already pointed out in [16, 17]. For example the environment could be at a lower temperature. In such a case, not the full energy spectrum of the environment is occupied if the width of the spectrum is much larger than k_BT, which changes the thermalization (and maybe also decoherence) process [18]. This is typically not the case for nuclear spins with small magnetic moments, but

in the case of a dense electronic environment the temperature of the latter could become important. Such effects will not be covered in this paper.

Regarding the set of all possible environmental states low temperatures are special. The overwhelming majority of all possible states we obtain by choosing a random state will be close to infinite temperature and behave the same, i.e. typically according to the concept of typicality [19–21]. For this reason the dynamics we will show for one single random state already represents the dynamics for most of all possible environmental states, cf. [14, 15, 22, 23].

All information about the dimer is contained in the reduced density matrix

$$\underset{\sim}{\rho} = Tr_E\left(\underset{\sim}{\rho}_{SE}\right), \tag{14}$$

in which $\underset{\sim}{\rho}_{SE} = |\psi\rangle\langle\psi|$ is the density matrix of the quantum state of the total system. Regarding the initial state Eq. (8) the reduced density matrix Eq. (14) describes a pure state, but becomes mixed over time through interactions $\underset{\sim}{H}_{SE}$. This process of entanglement is the essence of decoherence for an observer of the dimer [24, 25]. Written in the basis of the eigenstates of $\underset{\sim}{H}_S$, the reduced density matrix Eq. (14) contains non-diagonal interference terms which decay over time.

There are various ways of quantifying decoherence; for example purity $Tr\left(\underset{\sim}{\rho}^2\right)$ or the von Neumann entropy $S = -Tr\left(\underset{\sim}{\rho}\ln\underset{\sim}{\rho}\right)$ [26]. We decided to look directly at the relevant (depending on the scenario) non-diagonal elements of the reduced density matrix. The more entangled the system and environment are, the smaller the absolute value of these matrix elements becomes and the more quantum mechanical superpositions of the dimer are destroyed. Of course, superpositions and coherence still exist at the level of the complete state of the total system including the environment, but experimentally the measurement statistics of the dimer as a subsystem turns more and more into a classical mixture.

We want to point out that this entanglement and therefore the decay of the non-diagonal elements of the reduced density matrix in general do not require a substantial energy exchange between system and environment [27]. Imagine a product state such as Eq. (8) and the system in a superposition $|\psi_S\rangle = |\psi_{S_1}\rangle + |\psi_{S_2}\rangle$. The state Eq. (8) can then be written as

$$\begin{aligned}|\psi\rangle &= \frac{1}{\sqrt{2}}\left(|\psi_{S_1}\rangle + |\psi_{S_2}\rangle\right)\otimes|\psi_E\rangle \\ &= \frac{1}{\sqrt{2}}|\psi_{S_1}\rangle\otimes|\psi_E\rangle + \frac{1}{\sqrt{2}}|\psi_{S_2}\rangle\otimes|\psi_E\rangle\,.\end{aligned} \tag{15}$$

If the Hilbert space of the environment is very large, there will exist states $|\psi_{E'}\rangle$ which lie infinitesimally close in energy but are orthogonal to $|\psi_E\rangle$, $\langle\psi_E|\psi_{E'}\rangle = 0$. If the interaction between system and environment propagates the state Eq. (15) into

$$\rightarrow \quad \frac{1}{\sqrt{2}}|\psi_{S_1}\rangle\otimes|\psi_E\rangle + \frac{1}{\sqrt{2}}|\psi_{S_2}\rangle\otimes|\psi_{E'}\rangle \tag{16}$$

the energy distribution between system and environment has not changed, but the non-diagonal elements in the reduced density matrix that represent the superposition of $|\psi_{S_1}\rangle$ and $|\psi_{S_2}\rangle$ have completely decayed.

IV. CALCULATIONS

In all following calculations the external magnetic field is fixed to be $B = -1$ T. We investigate the behavior of the four different initial scenarios A, B, C and D described by equations (9), (10), (11) and (12). To begin with, we fix $\lambda = 1$ and vary the magnetic interaction strength $g\mu$ of the environmental spins, which affects both $\underset{\sim}{H}_{SE}$ and $\underset{\sim}{H}_E$.

In Figs. 5, 6 and 7 the absolute value of the relevant non-diagonal element $|\rho_{ij}|$ of the reduced density matrix Eq. (14) is shown. For scenario A this is $|\langle\psi^+_{Clock}|\,\underset{\sim}{\rho}\,|\psi^-_{Clock}\rangle|$, for scenario B it is $|\langle\psi^+_{Clock}|\,\underset{\sim}{\rho}\,|\downarrow\downarrow\rangle|$, for scenario C it is $|\langle\uparrow\uparrow|\,\underset{\sim}{\rho}\,|\downarrow\downarrow\rangle|$ and for scenario D it is $|\langle\psi^-_{Clock}|\,\underset{\sim}{\rho}\,|\downarrow\downarrow\rangle|$. These values decay through interactions with the environment $\underset{\sim}{H}_{SE}$, in most of the shown cases approximately exponentially. But for the weaker environments a Gaussian like decay is possible as also pointed out in [16].

Figs. 8, 9 and 10 show the associated real parts of these matrix elements. They oscillate with a frequency ω equal to the transition energy of the two $\underset{\sim}{H}_S$ eigenstates the superposition is built of (cf. Fig. 1). For scenarios A and D this is a much higher frequency than in scenarios B and C. Here we clearly see that the transition energy ω is not the most important parameter in the sense that it alone would set the timescale for decoherence. Scenario D has a much shorter decoherence time although it has almost the same ω as scenario A. We already pointed out that an energy transfer (relaxation) from system to environment or the other way around is not necessary for decoherence [27].

The timescale of decoherence is primarily given by the strength of $\underset{\sim}{H}_{SE}$. This part of the Hamiltonian depends linearly on the magnetic moments $g\mu$ of the environmental spins. In Figure 5 this parameter is chosen as $g\mu = 0.3359$ K/T, rising up to $g\mu = 0.6717$ K/T in Fig. 6 and to $g\mu = 1.3434$ K/T in Fig. 7. We find that in all these cases scenario A performs best regarding its decoherence time, but its advantage becomes drastically smaller when the environment couples stronger to the system (larger $g\mu$).

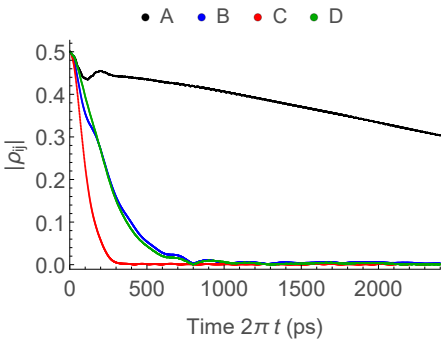

FIG. 5. Evolution of the absolute value of the relevant non-diagonal element $|\rho_{ij}|$ of the reduced density matrix Eq. (14) in the different scenarios A, B, C and D described in equations (9), (10), (11) and (12). The chosen parameters are $\lambda = 1$, $g\mu = 0.3359$ K/T and $B = -1$ T.

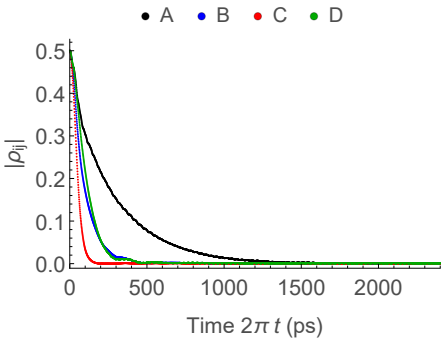

FIG. 6. Same as Fig. 5, but with $g\mu = 0.6717$ K/T.

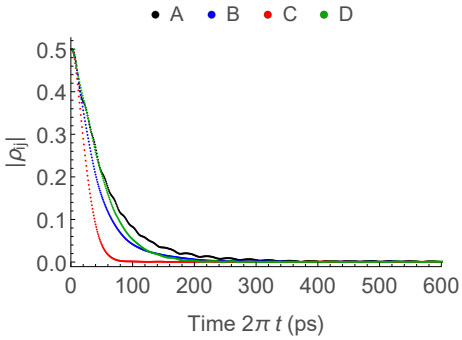

FIG. 7. Same as Fig. 5, but with $g\mu = 1.3434$ K/T and a shorter period of time.

Figures 11, 12 and 13 show time evolutions of initial scenario A for a lot of different values of λ and again different parameters $g\mu$. Here we see that λ, which scales the strength of the internal dynamic of the bath only, has a big impact on the decoherence behavior of the system. In case of a weak coupling between system and environment (Fig. 11) a large value of λ changes the decoherence behavior from approximately Gaussian to exponential.

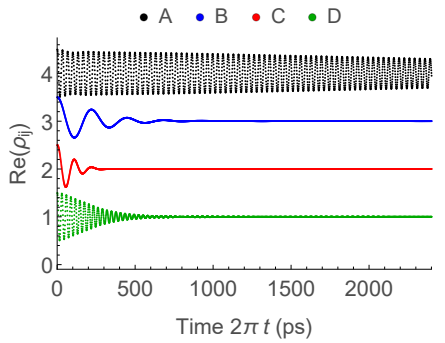

FIG. 8. Same as Fig. 5, but the real part of ρ_{ij} (with integer offsets) is shown instead of the absolute value. The oscillation frequency in the different scenarios A, B, C and D is given by the transition energies in Fig. 1. The amplitude of this oscillation is given by the absolute value of ρ_{ij}.

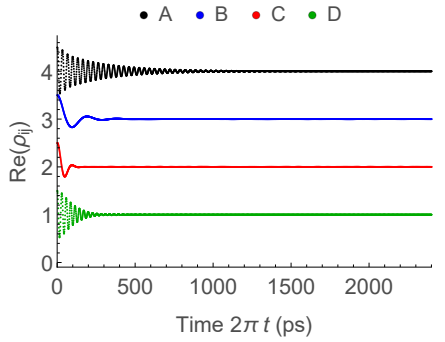

FIG. 9. Same as Fig. 8, but with $g\mu = 0.6717$ K/T.

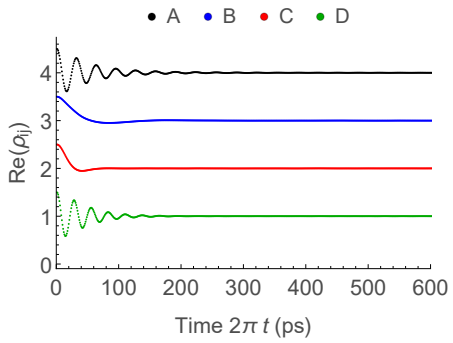

FIG. 10. Same as Fig. 8, but with $g\mu = 1.3434$ K/T and a shorter period of time.

Further increasing λ leads to an oscillating decoherence time in a certain range.

For a strong coupling between system and environment (Fig. 13) the decay is always exponential even if $\lambda = 0$, and in this regime the decoherence time can be significantly improved by increasing λ.

Another effect we see in all three figures is that for a small value of $\lambda \leq 1$ the decaying $|\rho_{ij}|$ has got a superimposed oscillation. In the case of the Gaussian decay, this

oscillation is distinctive right at the beginning, while in the exponential case it is visible at later times.

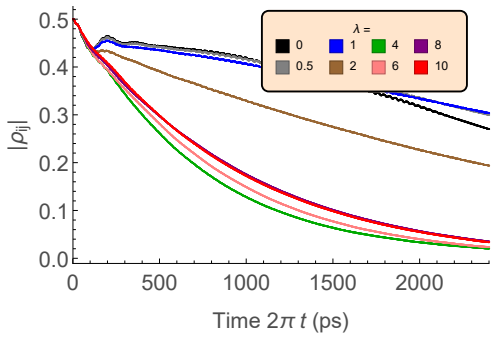

FIG. 11. Evolution of the absolute value of the relevant non-diagonal element $|\rho_{ij}|$ of the reduced density matrix Eq. (14) in initial scenario A for different scaling parameters λ and fixed parameters $g\mu = 0.3359$ K/T and $B = -1$ T. Increasing λ leads to a transition from Gaussian to exponential decay law.

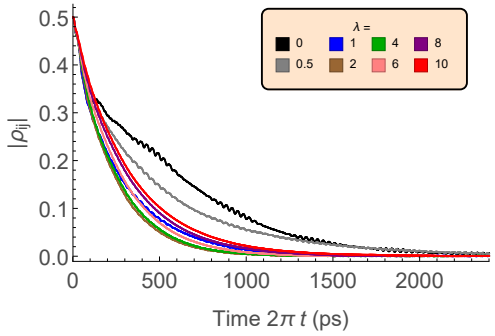

FIG. 12. Same as Fig. 11, but with $g\mu = 0.6717$ K/T.

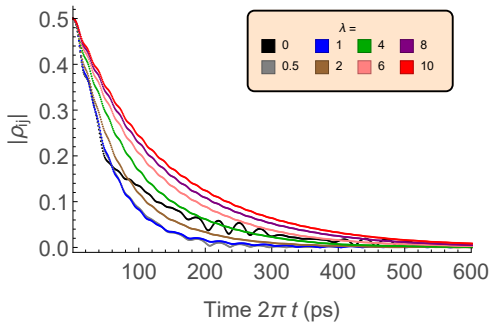

FIG. 13. Same as Fig. 11, but with $g\mu = 1.3434$ K/T and a shorter period of time. In this regime a stronger interaction between environmental spins leads to a relative increase of decoherence time with growing λ.

V. SUMMARY

In our investigation we study the decoherence of a single Heisenberg-coupled spin dimer interacting with a spin bath. We restrict ourselves to the effect of dipolar interactions on decoherence. Other sources of decoherence such as phonons [28] will be postponed to future investigations. We prepared the system in different initial states (A, B, C, and D) and find that indeed the clocklike superposition A has longer decoherence times than other initial scenarios. Our notion of decoherence time refers to a setting where a single dimer subject to a spin bath is investigated. This differs from usual investigations of decoherence, where T_2^* times characterize a dephasing ensemble.

The advantage of the clocklike scenario is impressive in a regime of a small coupling between system and environment. The difference between the scenarios is getting smaller with rising strength of this coupling. In the case of a weak coupling between system and environment the clock like superposition decays Gaussian if the internal bath interactions are small enough, otherwise the decay becomes exponential and the decoherence time gets much worse.

In the case of a strong coupling between system and environment the decay of superpositions is always exponential, even if the environmental spins do not interact with each other at all ($\lambda = 0$). One surprising result is that in this regime the decoherence time can be improved significantly by rising the internal interaction strength among the bath spins. A possible explanation using Fermi's golden rule might be that in this regime the smaller density of bath states leads to slower decoherence as it does equivalently for thermalization [29, 30]. The effect of a small density of bath states on decoherence needs to be further investigated, both theoretically and experimentally.

A final remark concerns the special arrangement of the environmental spins in our study. We studied several other arrangements, in particular also one, where all environmental spins are situated in the lower hemispheres around the dimer spins – a situation that appears to be more adapted to the experimental situation. However, our numerical experience yields that the various geometries change the decoherence of the system primarily through a different interaction strength between environmental spins (for a fixed distance between dimer and bath), which is covered in our model by choosing different factors λ.

ACKNOWLEDGMENT

This work was supported by the Deutsche Forschungsgemeinschaft DFG 355031190 (FOR 2692); 397300368 (SCHN 615/25-1)). P.V. thanks Lennart Dabelow for fruitful discussions and Kristel Michielsen, Hans De

Raedt, as well as Fengping Jin for helpful advise concerning advanced numerics.

[1] Y. Bae, K. Yang, P. Willke, T. Choi, A. J. Heinrich, and C. P. Lutz, "Enhanced quantum coherence in exchange coupled spins via singlet-triplet transitions," Science Advances **4**, eaau4159 (2018).

[2] L. Escalera-Moreno, A. Gaita-Ariño, and E. Coronado, "Decoherence from dipolar interspin interactions in molecular spin qubits," Phys. Rev. B **100**, 064405 (2019).

[3] M. Shiddiq, D. Komijani, Y. Duan, A. Gaita-Ariño, E. Coronado, and S. Hill, "Enhancing coherence in molecular spin qubits via atomic clock transitions," Nature **531**, 348 (2016).

[4] G. Wolfowicz, A. M. Tyryshkin, R. E. George, H. Riemann, N. V. Abrosimov, P. Becker, H.-J. Pohl, M. L. W. Thewalt, S. A. Lyon, and J. J. L. Morton, "Atomic clock transitions in silicon-based spin qubits," Nature Nanotechnology **8**, 561 (2013).

[5] H. De Raedt, B. Barbara, S. Miyashita, K. Michielsen, S. Bertaina, and S. Gambarelli, "Quantum simulations and experiments on Rabi oscillations of spin qubits: Intrinsic vs extrinsic damping," Phys. Rev. B **85**, 014408 (2012).

[6] A. Lunghi and S. Sanvito, "Electronic spin-spin decoherence contribution in molecular qubits by quantum unitary spin dynamics," J. Magn. Magn. Mater. **487**, 165325 (2019).

[7] J. Liu, J. Mrozek, W. K. Myers, G. A. Timco, R. E. P. Winpenny, B. Kintzel, W. Plass, and A. Ardavan, "Electric Field Control of Spins in Molecular Magnets," Phys. Rev. Lett. **122**, 037202 (2019).

[8] C. Godfrin, A. Ferhat, R. Ballou, S. Klyatskaya, M. Ruben, W. Wernsdorfer, and F. Balestro, "Operating Quantum States in Single Magnetic Molecules: Implementation of Grover's Quantum Algorithm," Phys. Rev. Lett. **119**, 187702 (2017).

[9] D. Stanek, C. Raas, and G. S. Uhrig, "Dynamics and decoherence in the central spin model in the low-field limit," Phys. Rev. B **88**, 155305 (2013).

[10] B. Lee, W. M. Witzel, and S. Das Sarma, "Universal Pulse Sequence to Minimize Spin Dephasing in the Central Spin Decoherence Problem," Phys. Rev. Lett. **100**, 160505 (2008).

[11] H. D. Raedt and K. Michielsen, "Computational Methods for Simulating Quantum Computers," ArXiv e-prints (2004), arXiv:0406210 [quant-ph].

[12] A. Haar, "Der Massbegriff in der Theorie der Kontinuierlichen Gruppen," Annals of Mathematics **34**, 147 (1933).

[13] B. Collins and P. Śniady, "Integration with Respect to the Haar Measure on Unitary, Orthogonal and Symplectic Group," Commun. Math. Phys. **264**, 773 (2006).

[14] C. Bartsch and J. Gemmer, "Dynamical Typicality of Quantum Expectation Values," Phys. Rev. Lett. **102**, 110403 (2009).

[15] P. Reimann, "Typical fast thermalization processes in closed many-body systems," Nat. Commun. **7**, 10821 (2016).

[16] S. Yuan, M. I. Katsnelson, and H. De Raedt, "Decoherence by a spin thermal bath: Role of spin-spin interactions and initial state of the bath," Phys. Rev. B **77**, 184301 (2008).

[17] F. Jin, K. Michielsen, M. A. Novotny, S. Miyashita, S. Yuan, and H. De Raedt, "Quantum decoherence scaling with bath size: Importance of dynamics, connectivity, and randomness," Phys. Rev. A **87**, 022117 (2013).

[18] E. J. Torres-Herrera and L. F. Santos, "Effects of the interplay between initial state and Hamiltonian on the thermalization of isolated quantum many-body systems," Phys. Rev. E **88**, 042121 (2013).

[19] J. Gemmer, M. Michel, and G. Mahler, *Quantum Thermodynamics: Emergence of Thermodynamic Behavior Within Composite Quantum Systems*, Lecture Notes in Physics, Vol. 784 (Springer, Berlin, Heidelberg, 2009).

[20] B. N. Balz, J. Richter, J. Gemmer, R. Steinigeweg, and P. Reimann, "Dynamical Typicality for Initial States with a Preset Measurement Statistics of Several Commuting Observables," in *Thermodynamics in the Quantum Regime: Fundamental Aspects and New Directions*, edited by F. Binder, L. A. Correa, C. Gogolin, J. Anders, and G. Adesso (Springer, Cham, 2018) pp. 413–433.

[21] P. Reimann and J. Gemmer, "Why are macroscopic experiments reproducible? Imitating the behavior of an ensemble by single pure states," Physica A , 121840 (2019).

[22] P. Reimann, "Dynamical typicality of isolated many-body quantum systems," Phys. Rev. E **97**, 062129 (2018).

[23] P. Reimann and L. Dabelow, "Typicality of Prethermalization," Phys. Rev. Lett. **122**, 080603 (2019).

[24] M. Schlosshauer, "Decoherence, the measurement problem, and interpretations of quantum mechanics," Rev. Mod. Phys. **76**, 1267 (2005).

[25] M. Schlosshauer, "The quantum-to-classical transition and decoherence," ArXiv e-prints (2014), arXiv:1404.2635 [quant-ph].

[26] H. C. Donker, H. D. Raedt, and M. I. Katsnelson, "Decoherence and pointer states in small antiferromagnets: A benchmark test," SciPost Phys. **2**, 010 (2017).

[27] A.-S. F. Obada, H. A. Hessian, and A.-B. A. Mohamed, "Entropies and entanglement for decoherence without energy relaxation in a two-level atom," Journal of Physics B: Atomic, Molecular and Optical Physics **40**, 2241 (2007).

[28] N. V. Prokof'ev and P. C. E. Stamp, "Theory of the spin bath," Rep. Prog. Phys. **63**, 669 (2000).

[29] R. Heveling, L. Knipschild, and J. Gemmer, "Compelling Bounds on Equilibration Times – the Issue with Fermi's Golden Rule," (2019), arXiv:1910.13262 [quant-ph].

[30] M. Schiulaz, E. J. Torres-Herrera, and L. F. Santos, "Thouless and relaxation time scales in many-body quantum systems," Phys. Rev. B **99**, 174313 (2019).